International Journal of Control, Automation and Systems 20(3) (2022) 941-955
http://dx.doi.org/10.1007/s12555-021-0099-8
ISSN:1598-6446 eISSN:2005-4092
http://www.springer.com/12555

Online Gait Generation Method Based on Neural Network for Humanoid Robot Fast Walking on Uneven Terrain

Haoran Zhong, Sicheng Xie, Xinyu Li, Liang Gao*, and Shengyu Lu

Abstract: Advanced humanoid robots highlight the ability of fast walking and adaptability to uneven terrain. However, owing to the complexity in walking dynamics, disturbances introduced by terrain height variations can adversely affect the bipedal walking performance. Moreover, to generate periodic gaits, most methods require to solve the gait generation problem by using nonlinear optimization approaches, resulting in difficulties for online control. To solve this problem, this paper proposes an online gait generation method to find periodic gaits for fast walking on uneven terrain by using a pre-trained neural network. First, to enhance the terrain adaptability, this paper proposes an improved walking pattern that allows the robots to skip the last single support phase. Such improvement enlarges the feasible step region when stepping down. A compensation strategy is also proposed to reduce the velocity tracking error. Then the improved whale swarm algorithm (IWSA) is applied to generate various datasets that cover the ranges of target velocities and terrain height variations. A back-propagation (BP) network is employed to train these datasets offline to learn the gait dynamics, which is further used to generate the optimal trajectories. Simulation results suggest that, compared with the current methods, the proposed method can solve the walking return map in a short time, with improvements in both maximum walking speed and terrain adaptability.

Keywords: Bipedal walking, humanoid robot, neural network, online gait generation, uneven terrain.

1. INTRODUCTION

In recent years, humanoid robots have been receiving increasing attention. Various robots have been successfully developed such as Atlas [1], DRC-Hubo [2], and DURUS [3]. These robots can accomplish diverse tasks and even remain stable when walking over snow-covered ground.

Inspired by previous research, we intend to develop a humanoid robot with high mobility, which demands both fast walking velocity and high terrain adaptability. Moreover, for online applications, the robot needs to cope with sudden changes in target velocity and terrain situation, therefore requiring a rapid gait generation in real-time. However, despite the progress in both theoretical research and application, online trajectory generation for fast bipedal walking over uneven terrain remains a tough task owing to the complexity in walking dynamics, the modeling errors in the real systems [4–6], and the disturbances introduced by the terrain height variations [7]. Moreover, the solving of gait generation problem brings considerable computational burden, which can deteriorate the robot response speed [8,9]. Although much efforts have been made to improve walking performance [7,10–13], it is still a challenging work to achieve both high mobility and flexibility in bipedal robots. Based on current researches, regular robots can barely reach a 2 m/s walking over a flat ground even under the simulation environment [11,15–17], which is far slower than the human of 4.97 m/s [18]. Such performance cannot meet our requirements. Therefore, in this study, we aim to develop an online gait generation method that can realize fast bipedal walking over uneven terrain. Based on our previous work in compliant control [19,20], we plan to use the spring-loaded inverted pendulum (SLIP) model to generate the trajectories.

The SLIP model is one of the most well-studied templates developed to describe fast and compliant locomotion [21–26]. It can effectively produce the center of mass (CoM) trajectories and ground reaction force (GRF) which are similar to those observed in human gaits [10, 27,28]. Moreover, compared to the linear inverted pendu-

Manuscript received February 5, 2021; revised April 25, 2021; accepted May 12, 2021. Recommended by Associate Editor Joonbum Bae under the direction of Editor Euntai Kim. This work was supported by the National Natural Science Foundation of China (grant number 51721092), and the program for the HUST Academic Frontier Youth Team (grant number 2017QYTD04).

Haoran Zhong, Sicheng Xie, Xinyu Li, and Shengyu Lu are with the State Key Laboratory of Digital Manufacturing Equipment and Technology, the School of Mechanical Science and Engineering, Huazhong University of Science and Technology (HUST), 1037, Luoyu Road, Hubei, Wuhan, China (e-mails: {1520098925, 592247127}@qq.com, lixinyu@hust.edu.cn, 1258206641@qq.com). Liang Gao is with the State Key Laboratory of Digital Manufacturing Equipment and Technology, the School of Mechanical Science and Engineering, Huazhong University of Science and Technology (HUST), 1037 Luoyu Road, Hubei,Wuhan, China (e-mail: gaoliang@mail.hust.edu.cn).
* Corresponding author.

lum model (LIPM) that ignores the leg compliance, the utilization of the SLIP model improves the robot performance in terrain adaption, impact absorption, and energy conservation at high speed [23,28–31]. With an added spring-like leg at the double support phase, Geyer *et al*. [23] extended this model to the bipedal walking field, that is, the Dual-SLIP model, and presented the possibility of analyzing both walking and running dynamics on the same basis. To cope with the uneven terrain, strategies that allow the robot to adjust the leg length have been proposed to compensate for the terrain variations [12,32,33]. However, these techniques inevitably introduce additional control variables that need to be determined. Some researchers consider the terrain height variations as disturbances [11,13], which are not appropriate for large terrain height variations. A more effective way is to consider the terrain condition when developing the dynamic model and solve the gait-finding problem [12,33]. In fact, continuous walking is normally modeled by the Poincare return map and discretized into numbers of single gait cycle [11,13,27,34]. During a cycle, current methods require the robot to experience single support, double support, and signal support phases in sequence and return to the initial posture [11,12,35,36]. Simple and effective as it is, such strategy also limits the feasible step region. For example, when stepping down, the robot cannot enter the last single support phase if the step length is too short, leading to an infeasible gait. Such limitation can bring negative effects to the gait finding procedure.

As discussed before, the computational burden is another issue that exists in most current methods. After the parametric modeling, the gait generation task is generally formulated as an optimization task with a group of unsolved control variables, such as touch-down angle and leg stiffness [30,37]. Some researchers used the evolutionary algorithm, e.g., differential evolution (DE) algorithm, genetic algorithm, and particle swarm optimization (PSO) algorithm, to optimize the parameters [38–44]. However, these methods require a long computing time that makes it difficult to realize an online tuning for robots. To reduce computing time, the most popular techniques are numerical methods, such as the fmincon function in Matlab/Optimization Toolbox [11–13,30]. These methods suffer from poor searching ability, and a lower cost time is not guaranteed. To realize online generation, tabular methods were proposed for fast gait generation [45,46]. The required parameters can be optimized off-line and restored in the look-up table. Unfortunately, the increase of input variables leads to an exponential growth of the table, which limits its practical application. Artificial neural network shows a strong ability of nonlinear information processing, and is gradually applied in bipedal walking [47–49]. Xin *et al*. [50] therefore attempted to solve the problem by using an artificial neural network to train the optimized datasets for running. The results suggest that the trained neural-network-based generator can effectively realize online gait generation for fast running with satisfying accuracy. However, the biped walking case was not discussed. Capi *et al*. [8] applied a Radial Basis Function Neural Network (RBFNN) based on a preset step length and step time, which is relatively not flexible. Nonetheless, neural networks have proven to be effective tools for realizing online gait generation [51–56].

To meet our requirements, we propose an improved neural-network-based gait generation method. To ameliorate the walking performance for uneven terrain, an improved walking pattern that allows the robot to autonomously skip the last single support phase is proposed. Such enhancement removes the step length restriction when stepping down. A velocity compensation strategy is also proposed for accurate speed tracking. Differs from previous researches that used fixed leg stiffness during a single step cycle [11,12,57], we allow the robot to adjust leg stiffness when entering the next phase. To realize online generation, a back propagation (BP) neural network is employed to learn the walking dynamics based on target and initial states, including both robot posture and velocity. The training datasets are generated by using the improved whale swarm algorithm (IWSA) [58], which is a powerful metaheuristic algorithm developed for the optimization task. The validity of the proposed method is confirmed by simulation experiments, in which both online and off-line walking performances in terms of maximum speed, tracking accuracy, and computing time are evaluated.

The contributions of this work include

1) Propose an improved walking pattern with a velocity compensation strategy that reduces speed tracking error and enlarges the feasible step region when stepping down.

2) Apply the IWSA algorithm to generate optimized gait datasets of high quality.

3) Employ a BP network-based control framework to realize online gait generation.

The remainder of this paper is organized as follows: The improved walking pattern with velocity compensation strategy is proposed in Section 2. The data generation and training procedures are presented in Section 3. Simulation experiments are conducted to verify the proposals in Section 4. Finally, the conclusion and future work are provided in Section 5.

2. TRAJECTORY OPTIMIZATION FOR UNEVEN TERRAIN

2.1. CoM trajectory implementation based on Dual-SLIP model

In this section, an improved walking pattern is proposed. First, the Dual-SLIP model considering the terrain height variations is developed. The proposed walking pattern is

then presented, and the gait finding issue is further converted to an optimization problem.

2.1.1 Improved walking pattern for uneven terrain

The conventional Dual-SLIP model consists of three phases [11], that is, the first single support phase SSA, the double support phase DS and the second support phase SSB, that is, the three-phase walking pattern, as shown in Fig. 1(a). In this study, 2D gait dynamics are developed. By considering the terrain height variations Δh, the CoM trajectory follows the basic spring-mass dynamics as

$$m\ddot{\mathbf{p}}_m = m\mathbf{g} + \sum_{i,j} k_i^j (l_0 + \Delta h - \|\mathbf{l}_i\|)\hat{\mathbf{e}}_{x,z}, \tag{1}$$

where m is the mass, k_i^j is the spring stiffness, in which $i \in \{\text{SSA, DS, SSB}\}$ represent the phase index, respectively, and $j \in \{\text{A, B}\}$ indicates the support and swing legs at the SSA phase, respectively. l0 is the rest length of the legs. $\hat{\mathbf{e}}_{x,z} = [0, 1]$ indicates the unit vectors in vertical and horizon directions. $\mathbf{p}_m = [m_x, m_z]$ is the CoM position, where m_x and m_z represent the coordinates at corresponding axes. $\mathbf{g}$ is the gravity vector. $\mathbf{l}_i$ denotes the leg vector. Both two legs contact the ground during the DS phase, whereas legs A and B contact the ground solely during SSA and SSB phases, respectively. Based on Fig. 1(a), xTD and θ represent the touchdown position and angle, respectively.

Generally, a single step sequentially experiences the three phases that are divided and triggered by two events: touch down (TD) and lift off (LO) events. The TD event suggests that the swing leg B contacts the ground and the walking state is transmitted from SSA to DS phase, whereas the LO event indicates that leg A lifts off from the ground and the walking state is transmitted from DS to SSB phase. Conventional methods require the robot to experience all three phases to perform a complete step, and a single gait cycle finishes when the CoM reaches the top

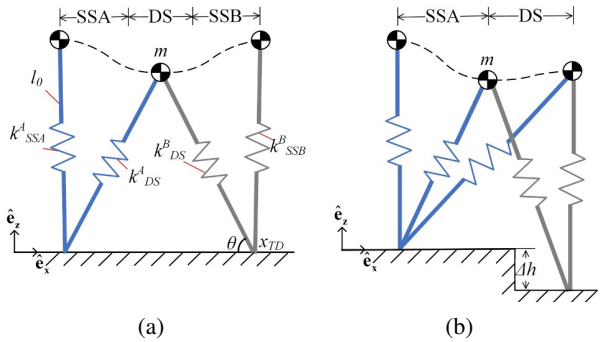

Fig. 1. Walking pattern. (a) Conventional walking pattern that experiences 3 phases; (b) Proposed walking pattern that allows skipping SSB phase to enhance flexibility.

of the contact point (that is, $m_x = x_{TD}$) [11,12,35]. However, for certain cases such as $\Delta h < 0$, LO event may not occur during the entire gait cycle. This condition occurs when the step length x_{TD} is too short under a certain Δh, as shown in Fig. 1(b), which can be described as follows:

$$\|l_A\| = \sqrt{(\|l_B\| - \Delta h)^2 + {x_{TD}}^2} < l_0, \tag{2}$$

where $\|\mathbf{l}_A\|$ and $\|\mathbf{l}_B\|$ represents the leg length of leg A and leg B. Normally, conventional methods consider such condition as an infeasible gait. However, the neglection of such condition can remarkably narrow the feasible region of step length, which brings a negative effect to the flexibility in robot walking. The limitation in the step region is expressed as

$$x_{TD} > \sqrt{{l_0}^2 - (\|l_B\| - \Delta h)^2}. \tag{3}$$

To remove such restriction, this study proposes a more flexible model that allows the robot to skip the SSB phase and moves to the next gait cycle. In this case, the robot only experiences two phases: SSA and DS phase, that is, the two-phase pattern. The robot can autonomously choose to experience three or two phases based on the current condition. The improved walking pattern is therefore developed.

The state at each phase is defined as

$$\text{SSA} = \{(\mathbf{p}_m, \dot{\mathbf{p}}_m) \mid \dot{m}_z < 0,\ m_z > z_{TD}\}, \tag{4}$$

where $z_{TD} = l_0 \sin(\theta) + \Delta h$ indicates the desired height of CoM when TD event occurs, and the beginning condition is $\dot{m}_{z0} = 0, m_{z0} = l_0$. The other two phases can be similarly defined as

$$\text{DS} = \{(\mathbf{p}_m, \dot{\mathbf{p}}_m) \mid \|\mathbf{l}_A\| < l_0 \text{ and } m_x < x_{TD}\}, \tag{5}$$

$$\text{SSB} = \{(\mathbf{p}_m, \dot{\mathbf{p}}_m) \mid \|\mathbf{l}_A\| = l_0,\ m_x < x_{TD}\}. \tag{6}$$

The phase transfer occurs when the corresponding event happens, which can be defined as

$$S_{TD} = S_{SSA \to DS} = \{(\mathbf{p}_m, \dot{\mathbf{p}}_m) \mid \dot{m}_z < 0,\ m_z = z_{TD}\}, \tag{7}$$

$$S_{LO} = S_{DS \to SSB} = \{(\mathbf{p}_m, \dot{\mathbf{p}}_m) \mid l_A = l_0 \text{ and } m_x < x_{TD}\}. \tag{8}$$

Especially, the proposed pattern allows a phase transfer from DS to the SSA phase in the next gait cycle, which can be described as

$$S_{DS \to SSA} = \{(\mathbf{p}_m, \dot{\mathbf{p}}_m) \mid l_A < l_0 \text{ and } m_x = x_{TD}\}. \tag{9}$$

The procedure of the improved walking pattern is shown in Fig. 2.

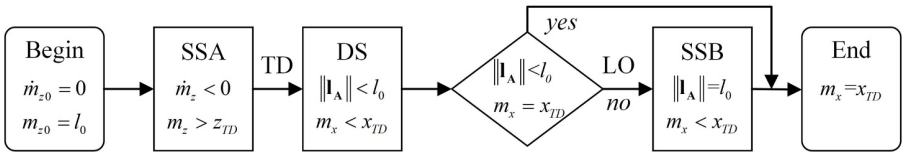

Fig. 2. The holistic procedure of the proposed walking pattern, which allows the robot to skip the SSB phase based on the current state. This characteristic can remove the step length limitations, therefore enlarging the feasible step region.

2.1.2 Periodic gait generation with velocity compensation

The control of the Dual-SLIP model can be implemented by analyzing the CoM motion at certain states. A typical discrete dynamic based on (1) can be described based on the Poincare return map as follows:

$$\mathbf{x}_{n+1} = P(\mathbf{x}_n, \mathbf{u}_n, \Delta h), \tag{10}$$

where $\mathbf{x}_n = [m_{xn}\ \ m_{zn}\ \ \dot{m}_{xn}\ \ \dot{m}_{zn}]$ denotes the initial state of CoM at the nth step, including the information of positions and velocities at xz plane. $\mathbf{x}_{n+1}$ represents both the final state and initial state at the nth and $n+1$th steps, respectively. $\mathbf{u}_n$ is the control variable matrix, and P represents the mapping from $\mathbf{x}_n$ to $\mathbf{x}_{n+1}$ according to (1). Therefore, one step gait can be implemented if an appropriate $\mathbf{u}_n$ is found that makes $\mathbf{x}_{n+1}$ follows the target state.

Previous researches have proven that the adjusting of leg stiffness and touch-down angle can effectively control the CoM motion [13,35]. Although current studies allow two legs to exhibit different compliance characteristics, the stiffness values are required to be fixed during a gait cycle, which can limit the maximum walking speed.

In this study, we remove such limitations and allows an adjustment to stiffness during different phases for each leg. The touch-down angle is also selected for control. Therefore, the control variable $\mathbf{u}$ is defined as

$$\mathbf{u} = [k^A_{SSA},\ k^A_{DS},\ k^B_{DS},\ k^B_{SSB},\ \theta], \tag{11}$$

where k^A_{SSA}, k^A_{DS}, k^B_{DS}, and k^B_{SSB} represent the corresponding leg stiffness values in corresponding phases, as shown in Fig. 1. Therefore, the periodic trajectory generation is formulated as an optimization problem that aims to determine appropriate $\mathbf{u}$ for the given initial state x_0, desired final state x_d, and terrain condition Δh as follows:

$$\begin{aligned} &\min_u \|\mathbf{x}_d - \mathbf{x}_m\| \\ &\text{s.t. } \|\mathbf{l}_A\| \le l_0,\ \|\mathbf{l}_B\| \le l_0,\ m_z > \Delta h,\ \dot{m}_x > 0, \end{aligned} \tag{12}$$

where the constraints limit the leg maximum length and ensure the CoM to move forward. $\mathbf{x}_d = [m_{zd}\ \dot{m}_{xd}\ \dot{m}_{zd}]$ denotes the desired final state. In this study, the step length control is not considered. $\mathbf{x}_m$ is the measured final state, which can be represented by

$$\mathbf{x}_m = P(\mathbf{x}_0,\ \mathbf{u},\ \Delta h). \tag{13}$$

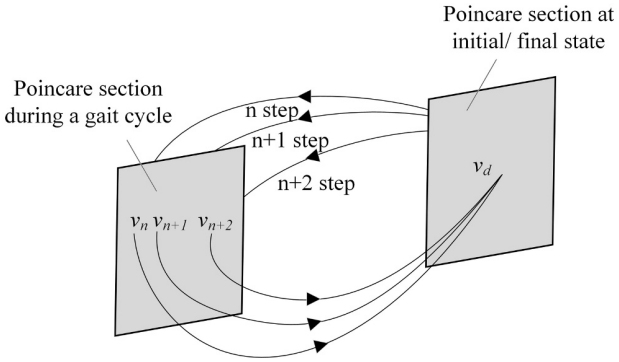

Fig. 3. Poincare return map for gait cycle. Conventional methods only focus on the initial and final states. However, the velocity during the middle state is uncontrollable therefore introducing unpredictable errors to the average velocity.

Another limitation that exists in current researches is they mainly focus on controlling the terminal velocity rather than the average speed. However, the velocity is varying during the step cycle, as shown in Fig. 3. This can introduce an adverse effect on the velocity tracking performance for multi-step gait generation owing to the cumulative error. In this study, we propose a velocity compensation strategy for accurate velocity control in continuous walking, in which the average speed of one step, rather than the terminal velocity, is controlled. The measured velocity for nth step, $\bar{v}^n$, is defined as

$$\bar{v}^n = {x_{TD}}^n / {t_f}^n, \tag{14}$$

where ${t_f}^n$ represents the time length of nth step. The measured final sate x_m is re-defined as

$$\mathbf{x}_m = P(x_0,\ \mathbf{u},\ \Delta h) = [m_{zf},\ \bar{v}_f,\ \dot{m}_{zf}], \tag{15}$$

where m_{zf} and $\dot{m}_{zf}$ are measured CoM position and velocity at z axis, respectively. $\bar{v}_f$ represent the measured average velocity. This strategy aims to regard one single step as a unity and regulate its average speed, which compensates for the cumulative error.

2.2. Trajectory optimization based on IWSA algorithm

In this section, the optimization problem of gait generation is solved by the IWSA algorithm. We first provide a

brief introduction to the IWSA algorithm. Then, the fitness function is constructed, and the optimization procedure is presented.

2.2.1 Introduction to IWSA algorithm

The IWSA algorithm is an effective metaheuristic algorithm proposed for optimization tasks. It contains a unique evaluation scheme that makes the search agents follow the guidance of their "better and nearest" members. In addition, a neighborhood searching strategy is adopted to enhance its local search ability and convergence rate. Previous researches have validated its superiority over traditional algorithms in terms of parameter optimization [58,59]. The evaluation procedure is described as follows:

$$X^* = X + rand(0,2) \cdot (Y - X), \tag{16}$$

where X^* and X denote the search agent in original and new positions. Y is the "better and nearest" member of X, indicating that Y has a better fitness value and stays closest to X. $rand(0,2)$ represents a uniformly distributed random number in a 0 to 2 range. For an individual X_i that stays in the current best position, no "better and nearest" members can be found. Therefore, it will search for the neighborhood area as follows:

$$X_i^* = X_i + rand(0.5,1) \cdot (X_j - X_k), \tag{17}$$

where $i \neq j \neq k$, and X_j and X_k denote the two nearest members to X_i. The details can be found in [44].

2.2.2 Fitness function development

Based on (12), the target final state x_d consists of two parts: a) the target posture parameters, including CoM height, m_{zd}, and its velocity at the vertical direction, $\dot{m}_{zd}$; and b) target velocity $\bar{v}_d$. Therefore, for the formulated problem, the fitness value, *fit*, can be defined as

$$\begin{aligned} fit =& \alpha_1 \cdot \|\bar{v}_f - barv_d\| + \alpha_2 \cdot \|m_{zf} - m_{zd}\| \\ &+ \alpha_3 \cdot \|\dot{m}_{zf} - \dot{m}_{zd}\|, \end{aligned} \tag{18}$$

where $[\alpha_1 \ \ \alpha_2 \ \ \alpha_3]$ is the matrix of weight factors. Since the posture errors can result in infeasible gait, thus drawing more of our concern. Therefore, the values are selected as $[2 \ \ 3 \ \ 1]$, which is constant.

In this study, the desired control variables are determined by using the IWSA algorithm. In this study, we require the robot to return to its initial posture at the terminal station. The initial and target posture is selected as $\dot{m}_{zf} = \dot{m}_{zd} = 0$, $m_{zf} = m_{zd} = l_0$.

2.2.3 Stop criterion

In this study, the optimum solution to this optimization problem is unknown. Therefore, we use the maximum iteration for the stop condition. In this case, the algorithm will stop when the predetermined maximum generation is reached.

2.2.4 Optimization procedure

The values of the control variable $u = [k_{SSA}^A, k_{DS}^A, k_{DS}^B, k_{SSB}^B, \theta]$ are used to represent the individuals in the population pool of the IWSA algorithm. Each parameter is normalized to 0 to 1 range before calculating the fitness value. After obtaining the optimized control parameters, the CoM trajectory can be easily acquired based on (1) using numerical approaches such as Runge-Kutta methods.

2.3. Foot trajectory planning

The previous section provides a way to obtain the appropriate control parameters as well as the desired CoM trajectory. In this section, the foot trajectory is obtained through a fifth-order Bézier Curve. It has the advantages of continuity, local controllability, and smooth curve, which can be expressed as follows [60]:

$$\mathbf{B}(t) = \sum_{i=0}^{n=5} \binom{n}{i} t^i (1-t)^{n-i} \mathbf{P}_i, \tag{19}$$

where t is the normalized time coefficient from 0 to 1. $\mathbf{B}(t)$ and $\mathbf{P}_i$ are the Bézier curve and selection point, respectively, which are of two dimensions (x and z) in this study. Owing to the proposed walking pattern that consists of two conditions, that is, three-phase pattern and two-phase pattern, the foot trajectory generation also requires to consider both these two patterns. After setting up certain conditions such as initial and final positions, as shown in Table 1, the Bézier curve is obtained.

In this study, to lower the contact impact and simplify the model, the foot movement in the ideal situation follows these assumptions:

1) the velocities at both x and z axes decrease to zero when contacting the ground.

Table 1. Initial and final states for foot trajectory generation.

	Initial state		Final state at each phase					
			SSA to DS		DS to SSB		DS to SSA	
axis	x	z	x	z	x	z	x	z
Leg A	m_{x0}	m_{z0}	m_{x0}	m_{z0}	$m_{x0} + x_{td}$	$m_{z0} + \Delta h + h_p$	m_{x0}	m_{z0}
Leg B	m_{x0}	$m_{z0} + h_p$	$m_{x0} + x_{td}$	$m_{z0} + \Delta h$	$m_{x0} + x_{td}$	$m_{z0} + \Delta h$	$m_{x0} + x_{td}$	$m_{z0} + \Delta h$

2) Considering the terrain height variations Δh, the height of peak point is set to $\Delta h + h_p$ to realize a smooth parabolic curve.
3) No collision occurs during the steps.
4) Foot-floor contact is without sliding.

In summary, the IWSA-based trajectory generation procedure follows:

1) Set up the population size $psize = 50$ initial state $\mathbf{x}_0$, desired final state $\mathbf{x}_d$, and maximum generation $Maxgen = 3000$.
2) Randomly generate an initial population group, and each individual contains control variables in the 0 to 1 range.
3) Conduct the IWSA algorithm, the fitness value is calculated based on (18).
4) Return to Step 3 unless the stop criterion is satisfied.
5) Obtained the CoM trajectory using the optimized control parameters based on (1).
6) Obtained the foot trajectory using the fifth-order B?zier Curve based on (19) and Table 1.
7) The final state is restored for the initial state for the next step.

Therefore, the IWSA-based off-line gait generator is developed for bipedal walking based on known terrain conditions.

3. DEVELOPMENT OF NEURAL NETWORK-BASED ONLINE GAIT GENERATOR

In this section, a neural network-based gait generator is developed to realize online trajectory generation. First, we introduce how to generate the datasets for training, and then present the structure of the developed neural network.

3.1. Training dataset generation

The basic idea of using a neural network is to generate the desired control variable matrix $\mathbf{u} = [k^A_{SSA}, k^A_{DS}, k^B_{DS}, k^B_{SSB}, \theta]$ based on terrain height variations Δh, the initial state $\mathbf{x}_0 = [m_{z0} \ \ \dot{m}_{x0} \ \ \dot{m}_{z0}]$, and the target final state $\mathbf{x}_d = [m_{zd} \ \ \dot{m}_{xd} \ \ \dot{m}_{zd}]$. Therefore, the input dataset $\mathbf{X}_{in}$ to the neural network is defined as $\mathbf{X}_{in} = [\mathbf{x}_0, \mathbf{x}_d, \Delta h]^T$. The validation dataset $\mathbf{Y}_{out}$ used for performance evaluation is described using the optimized control variable matrix as $\mathbf{Y}_{out} = \mathbf{u}$. A group of the training dataset is thus formulated.

In this study, we aim to generate a fast walking trajectory for uneven terrain. The velocity and terrain height variations range from 1 to 3 m/s and 0 to 0.2 m, respectively. Both the indices of maximum velocity and terrain height variations are higher than previous researches [11,12,61]. With a control accuracy of 0.05 m/s, 8405 groups of data can be used for training. However, small data size can result in overfitting or underfitting. In addition, 5% of the datasets are selected as the test sets. Compared to the current studies that check through all the feasible regions of control variables [50], the proposed method based on the IWSA algorithm is suggested to be more efficient and generate well-distributed data.

3.2. Training dataset generation

A BP neural network is developed to train the collected datasets, which consist of 4 hidden layers. The number of units per layer is set to be 32, 64, 64, 32. The general parameters of the network are listed in Table 2 and the BP network structure is shown in Fig. 4. The learning process of BP network can be described as follows:

$$W(n) = W(n-1) - \Delta W(n), \tag{20}$$

$$\Delta W(n) = \eta \frac{\partial E}{\partial W}(n-1) + \alpha \Delta W(n-1). \tag{21}$$

The output of the back-propagation network can be described as follows:

$$y_j = f(\sum_i w_{ji} x_i - \theta_j), \tag{22}$$

$$z_l = f(\sum_j v_{lj} y_j - \theta_l), \tag{23}$$

where x_i, y_i, and z_i represent the input node, the node of the hidden layer, and the node of the output layer respectively.

Table 2. BP network structure and settings.

Parameters	Values
Unit number in each hidden layer	32-64-64-32
Activation function in each hidden layer	relu
Learning rate	0.001
Optimizer	Adam
Batch size	128
Evaluation indicator	Mean-squared error

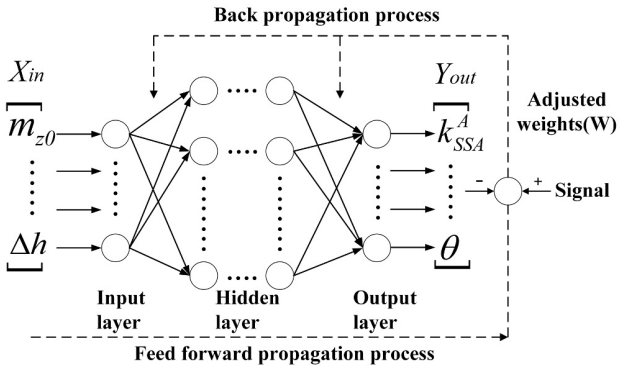

Fig. 4. BP neural network structure.

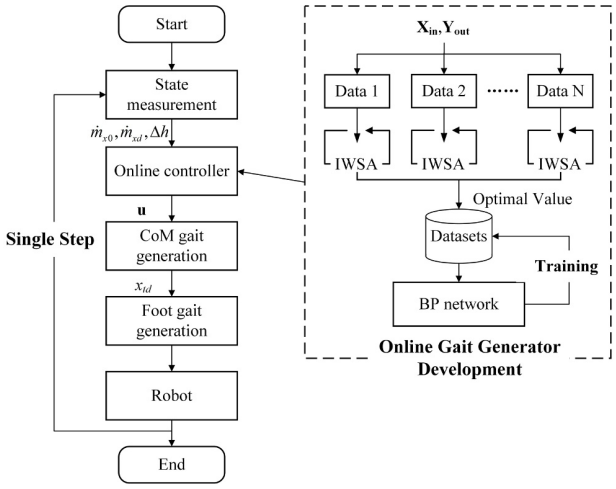

Fig. 5. Holistic online gait generation for fast walking on uneven terrain.

Table 3. Parameters selected for gait optimization.

Parameters	Definitions	Values
m	Mass	100 kg
l_0	Leg length	1 m
Δh	Terrain height variations	−0.02 to 0.02 m
k	Leg stiffness	10 to 50 kN/m
θ	Tough-down angle	5 to 85°
psize	Population	100
Maxgen	Maximum generation	3000
h_p	Ankle swing height	0.1 m

w_{ji} and v_{ji} represent the weight value. θ_j and θ_l represent the threshold. t_l is the expected value of the output node.

The learning rate can severely affect the performance of the trained model. Previous studies suggest that an appropriate learning rate can balance the convergence speed and model effectiveness [62]. In this study, the learning rate lr is experimentally set as 0.001. The mean-squared error *MSE* is used as the loss function, which is described as

$$MSE = \frac{1}{N}\sum_{i=1}^{N}(Y_{out} - f_{BP}(X_{in}))^2, \tag{24}$$

where f_{BP} represents the mapping relation of the BP network, and N denotes the dimension.

Fig. 5 shows the schematic diagram of the holistic online gait generation for fast walking on uneven terrain. First, the online gait generator needs to be developed. Based on the requirement, a group of $\mathbf{X}_{in}$ and $\mathbf{Y}_{out}$ are sent to generate the datasets by using IWSA. The optimized control variables are used to establish the training database, and the BP network is applied to learn from these data, therefore constructing the online gait generator. For online gait generation, based on the measured initial velocity, terrain condition, and target velocity, the optimal control variables and CoM trajectories can be generated by the developed online gait generator, and the foot trajectory can be planned based on the fifth-order Bézier Curve. Therefore, optimal one-step gaits are generated.

4. SIMULATION RESULTS AND DISCUSSION

4.1. Experimental setup

The experiments are performed in Matlab 2017b/Simulink software The IWSA-based optimization method proposed in Section 2 is applied to generate gaits of velocity ranges from 1 to 3 m/s. The parameters selected for optimization are listed in Table 3. The range of leg stiffness is selected according to human gaits [63]. In this study, the control of step length is not considered. The initial state $\mathbf{x}_0 = [m_{z0} \ \ \dot{m}_{x0} \ \ \dot{m}_{z0}]$ is set to $[l_0, v_{x0}, 0]$, and the target final state $\mathbf{x}_d = [m_{zd} \ \ \dot{m}_{xd} \ \ \dot{m}_{zd}]$ is set to $[l_0, v_{xd}, 0]$, where v_{x0} and v_{xd} are initial and desired velocities, respectively.

In this study, the fitness value, the velocity tracking error, the feasibility, and the computing time are used as the indexes to evaluate the effectiveness of the proposed method. We conduct four experiments as follows:

Experiment 1 (Maximum-speed walking experiments)**:** The initial and target velocities are set to 3 m/s, and the Δh is set to −0.2 m, −0.1 m, 0 m, 0.1 m, 0.2 m, respectively. Experiment 1 is designed to test the maximum speed of bipedal walking under various terrain conditions.

Experiment 2 (General variable-speed walking experiments)**:** The initial and target velocities range from 1 to 3 m/s. Experiment 2 is designed to evaluate the general performance of the optimization-based generation method with full-speed rang.

Experiment 3 (Online gait generation experiments)**:** Walking performances at both uniform and variable velocity are evaluated. In uniform-velocity walking, the initial and target velocities are set to 3 m/s; in variable-velocity walking, the target speed increases from 1 to 3 m/s. Δh is set to −0.2 m. The gaits are generated by using the off-line gait generator, non-compensated off-line gait generator, and neural-network-based online method. Experiment 3 is designed to evaluate the performance of the proposed online generation method under different speed conditions, in which the online generation method is compared to optimization-based and non-compensated generation methods to validate its effectiveness.

Experiment 4 (Verification experiment based on Webots platform)**:** The walking environment is constructed with height variations of ±0.2 m. The robot needs to walk continuously for 10 steps at a speed of 3 m/s. Experiment 4 is designed to evaluate the walking performance of the real robot in real scene. The virtual prototype of the designed robot is shown in Fig. 6 and Table 4.

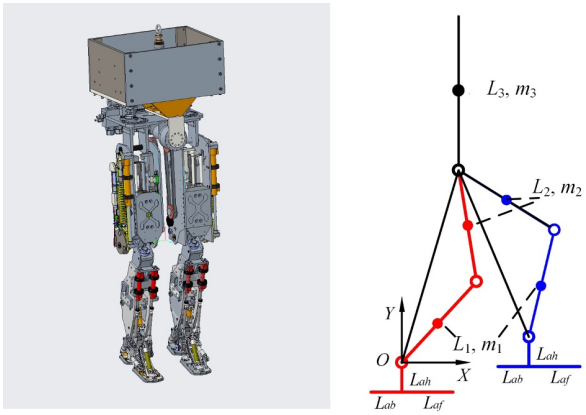

Fig. 6. The virtual prototype of biped robot.

Table 4. The parameters of the biped robot.

Parameter	value	Parameter	Value
g/m·s^{-2}	9.81	L_2/m	0.55
m_1/kg	14	L_3/m	0.8
m_2/kg	16	L_{ah}/m	0.115
m_3/kg	55	L_{ab}/m	0.125
L_1/m	0.55	L_{af}/m	0.205

4.2. Results and discussion

4.2.1 Maximum-speed walking evaluation experiments

Fig. 7 shows the optimized CoM and foot trajectories for terrain height changes from −0.2 to 0.2 m with a constant speed of 3 m/s. Based on Figs. 7(b) to 7(e), the CoM trajectories are consistent with those obtained by humans, that is, the CoM first drops to the lowest point in the first half step and then raises in the last half [11,64]. Under these conditions, the robot experiences all three phases. However, a different curve is presented in Fig. 7(a), in which the last single support phase SSB is not observed.

This is owing to the disturbance introduced by the large terrain height descent that prevents the swing leg (that is, leg A) from leaving the ground. In this case, the proposed walking pattern allows the robot to skip the SSB phase and prepare to enter the next step, which benefits flexibility. In terms of foot trajectories, we observe that smooth curves are obtained through the fifth-order Bzier Curve. The contact speed is restrained to 0 to reduce the impact. Moreover, the pre-set ankle swing height h_p is introduced to avoid the collision and realize a parabolic curve. Results from Fig. 7 validates the effectiveness of the proposed IWSA-based method to generate a fast walking gait that tolerates large known height variations (up to 20% of the leg length).

4.2.2 General variable-speed walking experiments

Table 5 shows the general performance of optimized gaits. The gaits obtained under the condition of flat terrain ($\Delta h = 0$) achieve better performance than those acquired on uneven terrain. Moreover, larger terrain height change leads to worse performance. The fitness values rise from 0.36 to 0.48 when Δh changes from 0.1 to 0.2 m. Under stepping down conditions ($\Delta h < 0$), by comparing results obtained by the proposed method with the conventional method, we observe that the former one performs better in terms of both maximum and average fitness values. Under the condition of $\Delta h = -0.2$ m, the proposed method aids to reduce the average fitness value from 0.43 to 0.37. The results obtained under the condition of $\Delta h = -0.1$ m indicate a similar performance. Besides, although results obtained conventional method at stepping up ($\Delta h > 0$) condition shows no distinct differences compared to those under the stepping down ($\Delta h < 0$) condition, smaller aver-

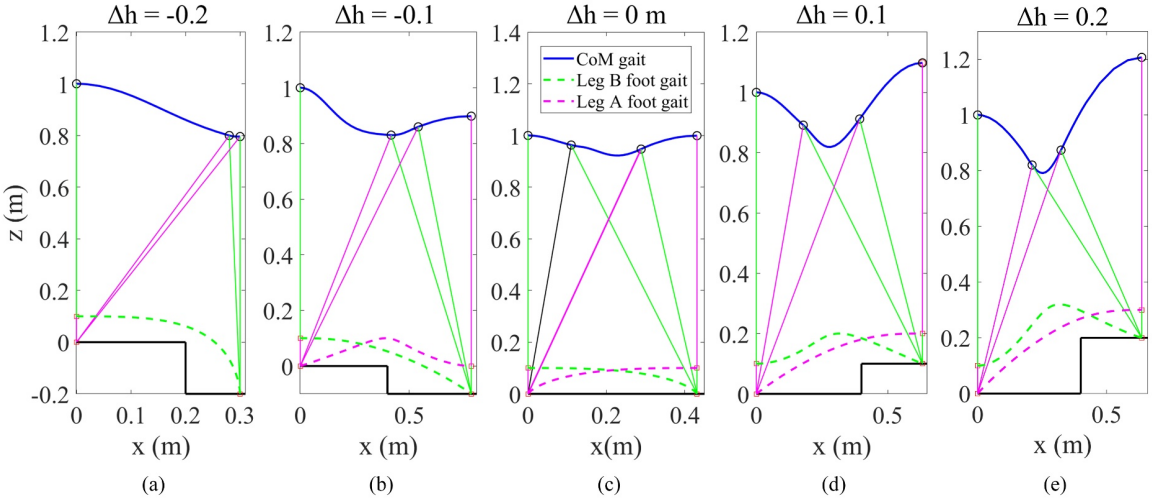

Fig. 7. The optimized CoM and foot trajectories for various terrain height variations (3 m/s). (a) $\Delta h = -0.2$ m; (b) $\Delta h = -0.1$ m; (c) $\Delta h = 0$ m; (d) $\Delta h = 0.1$ m; (e) $\Delta h = 0.2$ m.

Table 5. Results of optimized gaits.

Δh	−0.2		−0.1		0	0.1	0.2
	Proposed	Conventional	Proposed	Conventional			
Max. fit	1.46	1.70	1.42	2.26	1.42	1.52	1.80
Ave. fit	0.37	0.43	0.37	0.41	0.29	0.36	0.48
Inf. gait	0	125	0	125	0	0	0

* Max. fit: Maximum fitness value; Ave. fit: Averages fitness value; Inf. gait: Number of infeasible gaits; The proposed method indicates the proposed walking pattern that allows the robot to skip the SSB phase, while the conventional method requires to experience all three phases.

age fitness values can be achieved by using the proposed method when stepping down. Such improvements are owing to the improved walking pattern enlarges the feasible step region, which leads to better optimization results. The number of infeasible gaits also suggests that the requirement of experiencing all three phases can limit the maximum speed range. When stepping down, 125 sets of target velocity cannot be achieved by using the conventional method. That is, the maximum speed is restricted to 2.7 m/s.

Fig. 8 presents the comparison of results obtained with and without velocity compensation strategy. We can observe from this figure that the proposed velocity compensation strategy can effectively reduce the velocity tracking error. On the flat terrain, an 64.7% (from 0.51 to 0.18 m/s) improvement in average performances. Results from uneven terrain tests show are similar. With compensation, we can control the general step motion, rather than the final state. A more distinct effect is expected in multi-step gaits, in which the errors are accumulated. Based on the average results, the robot achieves the smallest error on the flat terrain, while the performance degrades when the terrain height variation increases. Moreover, the results obtained from the stepping down condition are better than those acquired from stepping up. The robot achieves 0.24 m/s tracking error when stepping down ($\Delta h = -0.2$ m), while this value increases to 0.35 m/s under stepping up ($\Delta h = 0.2$ m) condition. Such results are consistent with those in Table 5. As discussed before, this is owing to that when during stepping down, the proposed walking pattern not only eliminates the restriction on step length but also removes the constraints in the SSB phase, therefore benefiting the optimization procedure. Also, combined with Table 5, we observe that the average errors in posture and velocity are less than 10% with the consideration of the weighting factors. The posture error, however, is smaller than that of the velocity error. This is reasonable since we assign higher weight values to posture based on (18).

Fig. 9 presents the results of the average velocity tracking error of all generated gaits. This figure shows the influence of initial and target velocities on tracking accuracy. We observe that a larger change between initial and

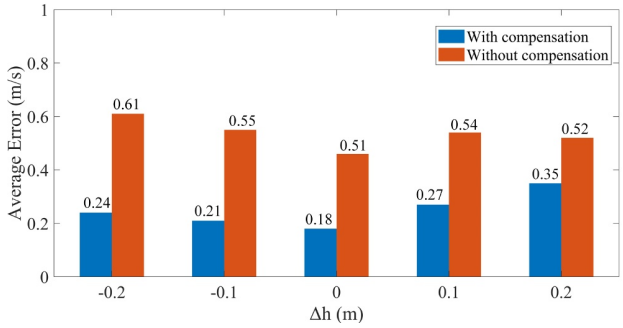

Fig. 8. The velocity tracking results, in which the initial and target velocities range from 1 to 3 m/s.

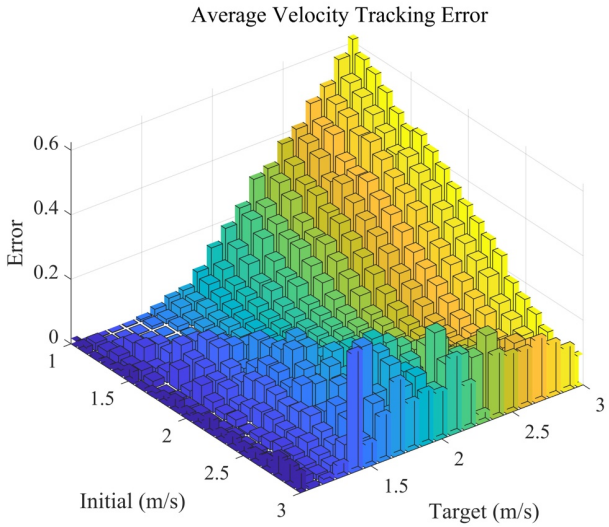

Fig. 9. The average velocity tracking error.

target velocities brings difficulties in control, resulting in larger errors. The largest error is obtained under such condition: initial velocity of 1 m/s and target velocity of 3 m/s. However, an acceleration condition (target velocity is higher than initial velocity) seems to achieves worse performance. This can be caused by the asymmetry in constraints. For example, the acceleration requires a higher stiffness in leg A during the DS phase. However, higher stiffness also leads to a fast speed at z axis, which vio-

lates the need of $\dot{m}_{zd} = 0$, therefore harming the optimization performance. Nonetheless, Fig. 9 suggests that small tracking errors under the condition of a velocity change within approximately 2 m/s. Moreover, higher accuracy can be achieved when tracking a constant velocity, even with fast speed up to 3 m/s.

4.2.3 Online gait generation experiment

BP network is developed to train the optimized gait datasets. After training, the *MSE* values of both training and testing datasets are less than 0.001, and the network is used to design the gait generator. Figs. 10 and 11 show the results of continuous walking under $\Delta h = 0.2$ m at constant and variable speeds, respectively. From these two figures, we observe that the condition of constant velocity achieves better results than the acceleration condition. Nonetheless, all three competitive methods can effectively generate gaits for 20 steps walking in the two cases. The IWSA-based method achieves the best results, while the non-compensated method performs the worst. Such results are consistent with those from Fig. 8, which further validates the effectiveness of the proposed velocity compensation strategy in continuous walking. In addition, compared with the IWSA-based off-line method, the results achieved by the BP network-based method distribute near the reference line, indicating a good fitting of the optimized datasets and the stability of continuous gaits. The observed deviations are tolerable, which are derived from the prediction error introduced by the BP network. The details are summarized in Table 6. Although the optimization method generates gaits that accurately track the target velocity, the large computational burden (computing time of 203.11 s) makes it hard to be applied for online control. By contrast, the proposed BP network-based gait generator can generate appropriate gaits within 0.03 s, which allows rapid regulation. Therefore, the proposed BP network-based gait generator provides a potential solution for online walking control of humanoid robots.

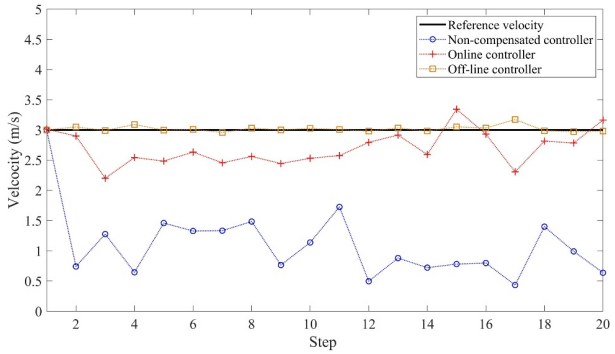

Fig. 10. Walking at a constant speed (3 m/s, $\Delta h = 0.2$ m)

.

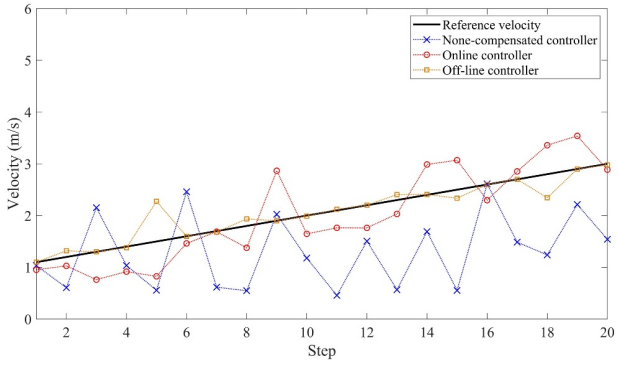

Fig. 11. Variable speed walking (acceleration condition, from 1 to 3 m/s, $\Delta h = 0.2$ m).

4.2.4 Verification experiments based on Webots platform

Fig. 12 provides the simulation environment, while Fig. 13 shows the side view of the second step. We can see that the step size of the robot becomes larger to adapt to the faster walking speed. When the swing leg touches down, the CoM shows an obvious rebound process, which is similar to human walking. During this process, the CoM momentum can be absorbed by changing the stiffness of the legs. In this way, the robot could avoid the rigid collision between the foot and the ground and realize stable walking. Fig. 14 shows the CoM trajectory of the biped robot. It can be seen that CoM can return to the preset position at the beginning and end of each step to avoid the accumulation of posture errors. The results show that the biped robot can smoothly pass through the complex terrain with continuous changing of height variations, showing good

Table 6. Results of continuous walking.

Method	Average error		Maximum error		Computing time/step [second]
	Constant velocity [m/s]	Acceleration [m/s]	Constant velocity [m/s]	Acceleration [m/s]	
Off-line gait generator	0.03	0.09	0.17	0.78	203.11
Non-compensated gait generator	2.57	0.93	1.90	1.95	201.06
Online gait generator	0.35	0.39	0.80	0.96	0.03

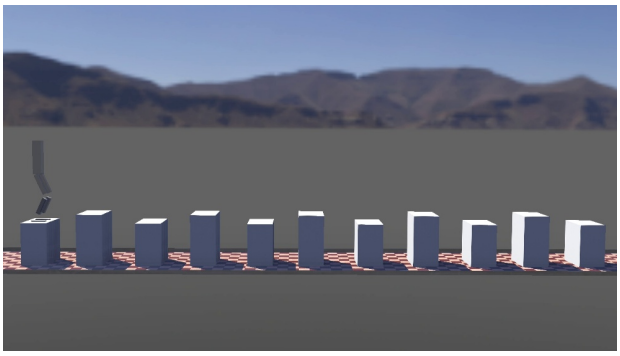

Fig. 12. The simulation environment.

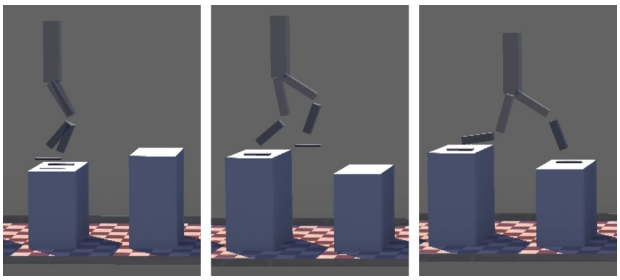

Fig. 13. The side view of the second step.

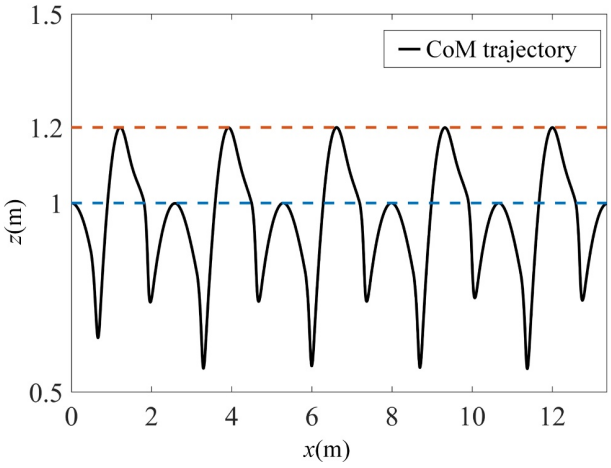

Fig. 14. The CoM trajectory during walking.

terrain adaptability. The results further verify the effectiveness of the proposed gait generation method.

4.2.5 Comparison with current methods

Table 7 shows a comparison of the proposed method with the current online generation method for bipedal walking on uneven terrain. For a fair comparison, the selected methods are all verified through simulations. The maximum velocity and tolerable Δh are derived either from the statement or experimental results in the corresponding paper. The method proposed in [11] is designed for walking over stairs, thus is more adaptive to higher terrain variations. Although the proposed method suffers a 38.3% loss in terrain adaptability (20% leg length compared to 32.4% leg length), it also achieves a 275% improvement (3 m/s compared to 0.8 m/s) in walking velocity. Therefore, the proposed method obtains a better achievement in the general performance, which can be beneficial to practical use. It should be pointed out that the computing time for the method proposed by Heydari and Farrokhi [14] is not clear. However, the authors indicated that they used *fmincon* function in Matlab to solve the gait generation problem, which is the same tool used by Liu *et al.* [12]. Therefore, we suggest that these two methods can achieve familiar performances in terms of computing time. Based on Table 7, we observe that the proposed method can achieve the highest velocity and lowest computing time. In terms of maximum tolerable Δh, the proposed method achieves the second best. In fact, as long as we reduce the target velocity to 2 m/s, the maximum tolerable Δh can increase to 30% leg length. The results of computing time for each step suggest that the neural network is much more efficient than the commonly used numerical method, which helps the robots to adapt to complicated and changeable environments. In conclusion, the proposed method fulfills our requirements in terms of both mobility and adaptability.

5. CONCLUSION AND FUTURE WORK

This study proposes a BP network-based online gait generation method for fast biped walking on uneven terrain. To improve walking performance when stepping down, an enhanced walking pattern is developed that allows the robot to skip the last single support phase SSB, which enlarges the feasible step region. A velocity compensation strategy is also proposed to reduce tracking errors in continuous walking. We apply the IWSA algorithm to generate gait datasets that cover the range of target ve-

Table 7. Performance comparison results.

Method	Maximum velocity [m/s]	Maximum tolerable Δh	Computing time/step [second]
Proposed method	**3**	**20 % leg length**	**0.03**
Hou *et al.* [10]	0.7	1.2 % leg length	0.38
Liu *et al.* [11]	1	6.0 % leg length	2.02
Heydari and Farrokhi [14]	0.8	32.4 % leg length	_____

locity and terrain height variations. A BP neural network is then developed to learn from these datasets and is further applied online to generate gaits for continuous walking. Simulation experiments are conducted to validate the proposals.

Based on the experimental results, we observe that: a) fast walking gaits up to 3 m/s on uneven terrain can be realized with smooth CoM and foot trajectories; b) the proposed walking pattern can improve walking performance when stepping down; and c) online walking control can be achieved by using the proposed method with tolerable performance loss. However, in this study, the step length is not a pre-set parameter that makes the foothold uncontrollable. Also, the actuator peak power constraint is not considered in this study. Such limitation can adversely affect the walking performance in real applications.

In future work, we plan to consider the step length control and apply the proposed method to real-world cases to further test its effectiveness.

REFERENCES

[1] G. Atmeh and K. Subbarao, "A neuro-dynamic walking engine for humanoid robots," *Robotics and Autonomous Systems*, vol. 110, pp. 124-138, September 2018.

[2] K. Sohn, "Optimization of vehicle mounting motions and its application to full-sized humanoid, DRC-Hubo," *Journal of Intelligent & Robotic Systems*, vol. 95, no. 1, pp. 19-46, April 2019.

[3] J. P. Reher, A. Hereid, S. Kolathaya, C. M. Hubicki, and A. D. Ames, "Algorithmic foundations of realizing multi-contact locomotion on the humanoid robot DURUS," *Algorithmic Foundations of Robotics XII*, pp. 400-415, Springer, May 2020.

[4] V. Stojanovic, S. He, and B. Zhang, "State and parameter joint estimation of linear stochastic systems in presence of faults and non-Gaussian noises," *International Journal of Robust and Nonlinear Control*, vol. 30, no. 16, pp. 6683-6700, August 2020.

[5] P. Cheng, S. He, V. Stojanovic, X. Luan, and F. Liu, "Fuzzy fault detection for Markov jump systems with partly accessible hidden information: An event-triggered approach," *IEEE Transactions on Cybernetics*, pp. 1-10, January 2021.

[6] Z. Chen, B. Zhang, V. Stojanovic, Y. Zhang, and Z. Zhang, "Event-based fuzzy control for TS fuzzy networked systems with various data missing," *Neurocomputing*, vol. 417, pp. 322-332, December 2020.

[7] Q. Li, Z. Yu, X. Chen, Q. Zhou, W. Zhang, L. Meng, and Q. Huang, "Contact force/torque control based on viscoelastic model for stable bipedal walking on indefinite uneven terrain," *IEEE Transactions on Automation Science and Engineering*, vol. 16, no. 4, pp. 1627-1639, October 2019.

[8] G. Capi, Y. Nasu, L. Barolli, and K. Mitobe, "Real time gait generation for autonomous humanoid robots: A case study for walking," *Robotics and Autonomous Systems*, vol. 42, no. 2, pp. 107-116, February 2003.

[9] W.-L. Ma, and A. D. Ames, "From bipedal walking to quadrupedal locomotion: Full-body dynamics decomposition for rapid gait generation," *Proc. of IEEE International Conference on Robotics and Automation (ICRA)*, pp. 4491-4497, May 2020.

[10] W. Q. Hou, T. H. Zhang, Y. Z. Chen, and H. X. Ma, "Compliant biped walking on uneven terrain with point feet," *International Journal of Advanced Robotic Systems*, vol. 13, no. 2, pp. 1-9, March 2016.

[11] Y. Liu, P. M. Wensing, D. E. Orin, and Y. F. Zheng, "Dynamic walking in a humanoid robot based on a 3D actuated Dual-SLIP model," *Proc. of IEEE International Conference on Robotics and Automation (ICRA)*, pp. 5710-5717, May 2015.

[12] Y. Liu, P. M. Wensing, D. E. Orin, and Y. F. Zheng, "Trajectory generation for dynamic walking in a humanoid over uneven terrain using a 3D-actuated dual-slip model," *Proc. of IEEE/RSJ International Conference on Intelligent Robots and Systems (IROS)*, pp. 374-380, September 2015.

[13] Y. Liu, P. M. Wensing, J. P. Schmiedeler, and D. E. Orin, "Terrain-blind humanoid walking based on a 3-D actuated Dual-SLIP model," *IEEE Robotics and Automation Letters*, vol. 1, no. 2, pp. 1073-1080, February 2016.

[14] R. Heydari and M. Farrokhi, "Robust model predictive control of biped robots with adaptive on-line gait generation," *International Journal of Control, Automation, and Systems*, vol. 15, no. 1, pp. 329-344, February 2017.

[15] F. Zhao and J. Gao, "Anti-slip gait planning for a humanoid robot in fast walking," *Applied Sciences*, vol. 9, no. 13, p. 2657, June 2019.

[16] S. Lohmeier, T. Buschmann, and H. Ulbrich, "Humanoid robot LOLA," *Proc. of IEEE International Conference on Robotics and Automation (ICRA)*, pp. 775-780, May 2009.

[17] J. Reher, W.-L. Ma, and A. D. Ames, "Dynamic walking with compliance on a cassie bipedal robot," *Proc. of 18th European Control Conference (ECC)*, pp. 2589-2595, June 2019.

[18] G. Pavei and A. La Torre, "The effects of speed and performance level on race walking kinematics," *Sport Sciences for Health*, vol. 12, no. 1, pp. 35-47, December 2016.

[19] H. Zhong, X. Li, and L. Gao, "Adaptive delay compensation for admittance control of hydraulic series elastic actuator," *Proc. of IEEE 16th International Conference on Automation Science and Engineering (CASE)*, pp. 384-389, August 2020.

[20] H. Zhong, X. Li, L. Gao, and H. Dong, "Position control of hydraulic series elastic actuator with parameter self-optimization," *Proc. of IEEE 4th International Conference on Advanced Robotics and Mechatronics (ICARM)*, pp. 42-46, July 2019.

[21] R. Blickhan, "The spring-mass model for running and hopping," *Journal of Biomechanics*, vol. 22, no. 11-12, pp. 1217-1227, February 1989.

[22] M. H. Raibert, "Legged robots that balance," *IEEE Expert*, vol. 1, no. 4, pp. 89-89, November 1986.

[23] H. Geyer, A. Seyfarth, and R. Blickhan, "Compliant leg behaviour explains basic dynamics of walking and running," *Proceedings of the Royal Society B: Biological Sciences*, vol. 273, no. 1603, pp. 2861-7, November 2006.

[24] E. Andrada, R. Blickhan, N. Ogihara, and C. Rode, "Low leg compliance permits grounded running at speeds where the inverted pendulum model gets airborne," *Journal of Theoretical Biology*, p. 110227, March 2020.

[25] T. Kobayashi, K. Sekiyama, Y. Hasegawa, T. Aoyama, and T. Fukuda, "Unified bipedal gait for autonomous transition between walking and running in pursuit of energy minimization," *Robotics and Autonomous Systems*, vol. 103, pp. 27-41, May, 2018.

[26] J. Seo, J. Kim, S. Park, and J. Cho, "A SLIP-based robot leg for decoupled spring-like behavior: Design and evaluation," *International Journal of Control, Automation, and Systems* vol. 17, no. 9, pp. 2388-2399, July 2019.

[27] M. N. Vu, J. Lee, and Y. Oh, "Control strategy for stabilization of the biped trunk-SLIP walking model," *Proc. of 14th International Conference on Ubiquitous Robots and Ambient Intelligence (URAI)*, pp. 1-6, June 2017.

[28] P. Zaytsev, T. Cnops, and C. D. Remy, "A detailed look at the SLIP model dynamics: Bifurcations, chaotic nehavior, and fractal basins of attraction," *Journal of Computational and Nonlinear Dynamics*, vol. 14, no. 8, August 2019.

[29] M. Shahbazi, R. Babuska, and G. A. D. Lopes, "Unified modeling and control of walking and running on the spring-loaded inverted pendulum," *IEEE Transactions on Robotics*, vol. 32, no. 5, pp. 1178-1195, October 2016.

[30] P. M. Wensing and D. E. Orin, "High-speed humanoid running through control with a 3D-SLIP model," *Proc. of IEEE/RSJ International Conference on Intelligent Robots and Systems (IROS)*, pp. 5134-5140, November 2013.

[31] M. Yazdani, H. Salarieh, and M. S. Foumani, "Bio-inspired decentralized architecture for walking of a 5-link biped robot with compliant knee joints," *International Journal of Control, Automation, and Systems*, vol. 16, no. 6, pp. 2935-2947, October 2018.

[32] X. Meng, Z. Yu, G. Huang, X. Chen, W. Qi, Q. Huang, and B. Su, "Walking control of biped robots on uneven terrains based on SLIP model," *Proc. of IEEE International Conference on Advanced Robotics and its Social Impacts (ARSO)*, pp. 174-179, October 2019.

[33] R. L. Galindo, E. Weimholt, and J. P. Schmiedeler, "Actuated dual-slip model of planar slope walking," *Proc. of ASME International Design Engineering Technical Conferences and Computers and Information in Engineering Conference (IDETC-CIE)*, pp. V05AT07A049, August 2019.

[34] M. Pogson, J. Verheul, M. A. Robinson, J. Vanrenterghem, and P. Lisboa, "A neural network method to predict task- and step-specific ground reaction force magnitudes from trunk accelerations during running activities," *Medical Engineering & Physics*, vol. 78, pp. 82-89, April 2020.

[35] H. R. Vejdani, A. Wu, H. Geyer, and J. W. Hurst, "Touchdown angle control for spring-mass walking," *Proc. of IEEE International Conference on Robotics and Automation (ICRA)*, pp. 5101-5106, May 2015.

[36] H. M. Joe and J. H. Oh, "A robust balance-control framework for the terrain-blind bipedal walking of a humanoid robot on unknown and uneven terrain," *Sensors*, vol. 19, no. 19, October 2019.

[37] I. Uyanık, *Adaptive Control of a One-legged Hopping Robot Through Dynamically Embedded Spring-loaded Inverted Pendulum Template*, Bilkent University, 2011.

[38] I. S. Kim, Y. J. Han, and Y. D. Hong, "Stability control for dynamic walking of bipedal robot with real-time capture point trajectory optimization," *Journal of Intelligent & Robotic Systems*, vol. 96, no. 3-4, pp. 345-361, December 2019.

[39] T. T. Huan, C. V. Kien, H. P. H. Anh, and N. T. Nam, "Adaptive gait generation for humanoid robot using evolutionary neural model optimized with modified differential evolution technique," *Neurocomputing*, vol. 320, pp. 112-120, December 2018.

[40] W. Suliman, C. Albitar, and L. Hassan, "Optimization of central pattern generator-based torque-stiffness-controlled dynamic bipedal walking," *Journal of Robotics*, vol. 2020, January 2020.

[41] C. Niehaus, T. Röfer, and T. Laue, "Gait optimization on a humanoid robot using particle swarm optimization," *Proc. of the 2nd Workshop on Humanoid Soccer Robots in Conjunction with 7th IEEE-RAS International Conference on Humanoid Robots*, pp. 1-7, November 2007.

[42] E.-S. Kim, M.-S. Kim, J.-Y. Choi, S. W. Kim, and J.-W. Kim, "Trajectory generation schemes for bipedal ascending and descending stairs using univariate dynamic encoding algorithm for searches (uDEAS)," *International Journal of Control, Automation, and Systems* vol. 8, no. 5, pp. 1061-1071, October 2010.

[43] D. Pršić, N. Nedić, and V. Stojanović, "A nature inspired optimal control of pneumatic-driven parallel robot platform," *Proc. of the Institution of Mechanical Engineers, Part C: Journal of Mechanical Engineering Science*, vol. 231, no. 1, pp. 59-71, August 2016.

[44] V. Stojanovic, N. Nedic, D. Prsic, L. Dubonjic, and V. Djordjevic, "Application of cuckoo search algorithm to constrained control problem of a parallel robot platform," *The International Journal of Advanced Manufacturing Technology*, vol. 87, no. 9, pp. 2497-2507, March 2016.

[45] M. H. Raibert and F. C. Wimberly, "Tabular control of balance in a dynamic legged system," *IEEE Transactions on Systems, Man, and Cybernetics*, no. 2, pp. 334-339, March 1984.

[46] Z. Song, L. Gao, and C. Hu, "A gait planning method for humanoid robot to step over discrete terrain," *Proc. of 5th International Conference on Advanced Robotics and Mechatronics (ICARM)*, pp. 507-512, December 2020.

[47] M. H. Sarajchi, S. Ganjefar, S. M. Hoseini, and Z. Shao, "Adaptive controller design based on predicted time-delay for teleoperation systems using Lambert W function," *International Journal of Control, Automation, and Systems*, vol. 17, pp. 1445-1453, May 2019.

[48] S. Ganjefar, M. Afshar, M. H. Sarajchi, and Z. Shao, "Controller design based on wavelet neural adaptive proportional plus conventional integral-derivative for bilateral teleoperation systems with time-varying parameters," *International Journal of Control, Automation, and Systems*, vol. 16, pp. 2405-2420, September 2018.

[49] S. Ganjefar, M. H. Sarajchi, S. M. Hoseini, and Z. Shao, "Lambert W function controller design for teleoperation systems," *International Journal of Precision Engineering and Manufacturing*, vol. 20, pp. 101-110, February 2019.

[50] S. Xin, B. Delhaisse, Y. You, C. Zhou, M. Shahbazi, and N. Tsagarakis, "Neural-network-controlled spring mass template for humanoid running," *Proc. of IEEE/RSJ International Conference on Intelligent Robots and Systems (IROS)*, pp. 1725-1731, October 2018.

[51] C. Aguilar-Ibanez and M. S. Suarez-Castanon, "A trajectory planning based controller to regulate an uncertain 3D overhead crane system," *International Journal of Applied Mathematics and Computer Science*, vol. 29, no. 4, pp. 693-702, December 2019.

[52] J. R. García-Sánchez, S. Tavera-Mosqueda, R. Silva-Ortigoza, V. M. Hernández-Guzmán, J. Sandoval-Gutiérrez, M. Marcelino-Aranda, H. Taud, and M. Marciano-Melchor, "Robust switched tracking control for wheeled mobile robots considering the actuators and drivers," *Sensors*, vol. 18, no. 12, pp. 1-21, December 2018.

[53] D. I. Martinez, J. J. Rubio, T. M. Vargas, V. Garcia, G. Ochoa, R. Balcazar, D. R. Cruz, A. Auilar, J. F. Novoa, and C. Aguilar-Ibañez, "Stabilization of robots with a regulator containing the sigmoid mapping," *IEEE Access*, vol. 8, pp. 89479-89488, April 2020.

[54] D. I. Martinez, J. J. Rubio, A. Aguilar, J. Pacheco, G. J. Gutierrez, V. Garcia, T. M. Vargas, G. Ochoa, D. R. Cruz, and C. F. Juarez, "Stabilization of two electricity generators," *Complexity*, vol. 2020, Article ID 8683521, December 2020.

[55] J. J. Rubio, G. Ochoa, D. Mujica-Vargas, E. Garcia, R. Balcazar, I. Elias, D. R. Cruz, C. F. Juarez, A. Aguilar, and J. F. Novoa, "Structure regulator for the perturbations attenuation in a quadrotor," *IEEE Access*, vol. 7, pp. 138244-138252, September 2019.

[56] J. O. Escobedo-Alva, E. C. Garcia-Estrada, L. A. Paramo-Carranza, J. A. Meda-Campaña, and R. Tapia-Herrera, "Theoretical application of a hybrid observer on altitude tracking of quadrotor losing GPS signal," *IEEE Access*, vol. 6, pp. 76900-76908, November 2018.

[57] L. C. Visser, S. Stramigioli, and R. Carloni, "Robust bipedal walking with variable leg stiffness," *Proc. of 4th IEEE RAS & EMBS International Conference on Biomedical Robotics and Biomechatronics (Biorob)*, pp. 1626-1631, June 2012.

[58] H. Zhong, C. Hu, X. Li, L. Gao, B. Zeng, and H. Dong, "Kinematic calibration method for a two-segment hydraulic leg based on an improved whale swarm algorithm," *Robotics and Computer-integrated Manufacturing*, vol. 59, pp. 361-372, May 2019.

[59] B. Zeng, X. Li, L. Gao, Y. Zhang, and H. Dong, "Whale swarm algorithm with the mechanism of identifying and escaping from extreme points for multimodal function optimization," *Neural Computing and Applications*, no. 32, pp. 5071–5091, April 2018.

[60] T. Sugiyama and N. Kamamichi, "Experimental verification of motion pattern generation for peristaltic mobile robot using numerical optimization method," *Proc. of Bioinspiration, Biomimetics, and Bioreplication X*, p. 113740U, April 2020.

[61] H. Lim and S. Park, "A bipedal compliant walking model generates periodic gait cycles with realistic swing dynamics," *Journal of Biomechanics*, vol. 91, pp. 79-84, June 2019.

[62] X. M. Ruan, Y. Y. Zhu, J. Li, and Y. Cheng, "Predicting the citation counts of individual papers via a BP neural network," *Journal of Informetrics*, vol. 14, no. 3, August 2020.

[63] H. Geyer, A. Seyfarth, and R. Blickhan, "Spring-mass running: Simple approximate solution and application to gait stability," *Journal of Theoretical Biology*, vol. 232, no. 3, pp. 315-328, February 2005.

[64] J. E. Zachazewski, P. O. Riley, and D. E. Krebs, "Biomechanical analysis of body mass transfer during stair ascent and descent of healthy subjects," *Journal of Rehabilitation Research and Development*, vol. 30, pp. 412-412, 1993.

Haoran Zhong received his B.S. degree from East China University of Science and Technology (ECUST), Shanghai, China, in 2014. He is now a Doctoral Candidate with the Department of Industrial and Manufacturing Systems Engineering, State Key Laboratory of Digital Manufacturing Equipment and Technology, School of Mechanical Science and Engineering, Huazhong University of Science and Technology (HUST). His current research interests include humanoid robot, series elastic actuator (SEA), and intelligent algorithms.

Sicheng Xie received his B.S. degree in mechanical engineering from the Huazhong University of Science and Technology (HUST), Wuhan, China, in 2019. He is now a Doctoral Candidate with the Department of Industrial and Manufacturing Systems Engineering, State Key Laboratory of Digital Manufacturing Equipment and Technology, School of Mechanical Science and Engineering, Huazhong University of Science and Technology (HUST). His current research interests include humanoid robot and gait planning.

Xinyu Li received his Ph.D. degree in industrial engineering from the Huazhong University of Science and Technology (HUST), Wuhan, China, in 2009. He is currently a Professor with the Department of Industrial and Manufacturing Systems Engineering, State Key Laboratory of Digital Manufacturing Equipment and Technology, School of Mechanical Science and Engineering, HUST. He has authored more than 80 refereed articles. His research interests include intelligent algorithm, big data, and machine learning.

Liang Gao received his Ph.D. degree in mechatronic engineering from the Huazhong University of Science and Technology (HUST), Wuhan, China, in 2002. He is currently a Professor with the Department of Industrial and Manufacturing System Engineering, State Key Laboratory of Digital Manufacturing Equipment and Technology, School of Mechanical Science and Engineering, HUST. He has authored more than 170 refereed articles. His research interests include operations research and optimization, big data, and machine learning.

Shengyu Lu received his M.Eng. degree in mechanical engineering from the Huazhong University of Science and Technology (HUST), Wuhan, China, in 2019. He is now a Doctoral Candidate with the Department of Industrial and Manufacturing Systems Engineering, State Key Laboratory of Digital Manufacturing Equipment and Technology, the School of Mechanical Science and Engineering, Huazhong University of Science and Technology (HUST). His current research interests include humanoid robot design and gait planning.